[3]M. Inoue and V. Toyozawa, J. Phys. Soc. Japan 20, 363 (1965).
[4]M. C. Teich, J. M. Schroeer, and G. J. Wolga, Phys. Rev. Letters 13, 611 (1964); H. Sonnenberg, H. Heffner, and W. Spicer, Appl. Phys. Letters 5, 95 (1964).
[5]E. M. Logothetis and P. L. Hartman, Bull. Am. Phys. Soc. 12, 273 (1967); Phys. Rev. Letters 18, 581 (1967).
[6]E. M. Logothetis, thesis, Cornell University, 1967, to be published.
[7]K. Teegarden and G. Baldini, Phys. Rev. 155, 896 (1967).
[8]R. J. Elliot, Phys. Rev. 108, 1384 (1957).
[9]J. Eby, K. Teegarden, and D. Dutton, Phys. Rev. 116, 1099 (1959).
[10]J. Taylor and P. L. Hartman, Phys. Rev. 113, 1421 (1959).
[11]W. E. Spicer, Phys. Letters 20, 326 (1966), and references therein.
[12]Such measurements were done on several solids with the 3.57-eV laser radiation (Ref. 6).

DYNAMICAL THEORY OF LOW-ENERGY ELECTRON DIFFRACTION

F. Hofmann and Harold P. Smith, Jr.
Space Sciences Laboratory, University of California, Berkeley, California
(Received 31 October 1967)

I. Introduction.—It has been shown by several authors[1-3] that the simple kinematical theory is inadequate for the detailed description of low-energy electron-diffraction (LEED) intensities as functions of electron energy. This is mainly due to the fact that scattering cross sections are large and, hence, multiple scattering is important. Dynamical effects in LEED (i.e., multiple scattering) have been treated by Hirabayashi and Takeishi[4] using a modified von Laue method, and by McRae[3] whose theory is based on Lax's self-consistent field formalism. In this Letter, we present an alternative dynamical theory for the calculation of LEED intensities.

II. The model.—Our model has the following properties: (1) The primary beam of electrons is represented by a plane wave.

(2) The crystal extends over the entire infinite half-space $z<0$ [i.e., the crystal surface is a plane $(z=0)$].

(3) Within the crystal, the potential is perfectly periodic in three dimensions.

(4) The majority of (elastically scattered) electrons traveling away from the crystal are contained in a number of discrete "beams." Experimental data show that this assumption is generally true in the energy range we are considering. (The spots in the diffraction pattern are bright compared with the background.)

One of the basic limitations of the model described above is the fact that surface anomalies in the crystal lattice cannot be taken into account. However, the model is still somewhat more general than the one used by McRae[3] because we do not assume the potential to be of the "muffin-tin" variety, and it is also more general than the Hirabayashi model since we do not restrict ourselves to the "two-beam" approximation.

III. Theory.—We start from the standard Bethe theory[5] in which the potential function $W(\vec{r})$ is expanded as

$$W(\vec{r})=\sum_{p,q,s} w_{p,q,s}\exp(2\pi i\vec{g}_{p,q,s}\cdot\vec{r}), \qquad (1)$$

where $\vec{g}_{p,q,s}=p\vec{b}_1+q\vec{b}_2+s\vec{b}_3$, and the $\vec{b}$'s define the unit cell of the reciprocal lattice. The real part of $W(\vec{r})$ gives rise to elastic scattering, whereas the imaginary part is used to simulate inelastic scattering.

The wave function ψ in the crystal is written in the form

$$\psi(\vec{r})=\sum_{l,m,n}\psi_{l,m,n}\exp(i\vec{k}_{l,m,n}\cdot\vec{r}), \qquad (2)$$

where $\vec{k}_{l,m,n}=\vec{k}_0+2\pi\vec{g}_{l,m,n}$, and $\vec{k}_0$ is a vector whose components are determined by the boundary conditions. The coefficients $\psi_{l,m,n}$ are then subject to a set of compatibility conditions[5]

$$\psi_{l,m,n}(K^2-k_{l,m,n}^2)+\sum_{p,q,s} w_{p,q,s}\psi_{l-p,m-q,n-s}=0, \qquad (3)$$

which are a direct consequence of the fact that $\psi(\vec{r})$ must be a solution of the Schrödinger equation, $\nabla^2\psi+(K^2+W)\psi=0$. K is the magnitude of the propagation vector of the primary electron beam.

According to property (4) of the model, the

wave function Φ in the vacuum is written as

$$\Phi(\vec{r}) = \sum_{l,m,n} \Phi_{l,m,n} \exp(i\vec{h}_{l,m,n} \cdot \vec{r}), \quad (4)$$

where $|\vec{h}_{l,m,n}| = K$.

With the assumption that the crystal surface ($z = 0$) coincides with one of the crystallographic planes (i.e., 100, 110, 111, etc.), it is easy to show that the surface boundary conditions can be stated as

$$\sum_n \Phi_{l,m,n} = \sum_n \psi_{l,m,n}, \quad (5)$$

$$\sum_n \Phi_{l,m,n} (\vec{h}_{l,m,n} \cdot \vec{1}_z) = \sum_n \psi_{l,m,n} (\vec{k}_{l,m,n} \cdot \vec{1}_z), \quad (6)$$

where $\vec{1}_z$ is a unit vector in the z direction. The sums on the left-hand side of Eqs. (5) and (6) involve only two terms, corresponding to the two solutions of the equation $|\vec{h}_{l,m,n}| = K$.

Furthermore, one finds that the real parts of the x and y components of $\vec{k}_0$ are determined by the direction of the incident electron beam, whereas their imaginary parts must be zero, due to the boundary conditions at infinity. The z component of $\vec{k}_0$ is a complex number whose imaginary part is negative because $|\psi(\vec{r})|$ must approach zero as z approaches $-\infty$.

The problem now consists of solving the sets of equations (3), (5), and (6). These equations cannot be solved exactly if the sums are terminated at a finite number of terms. However, an approximate solution can be obtained in the following way: From Eq. (3) it is clear that the $\psi_{l,m,n}$'s with large indices must be small. In fact, an actual calculation (Fig. 1) shows that all $\psi_{l,m,n}$'s which lie outside the Ewald sphere and whose distance from the surface of that sphere is more than a few reciprocal lattice spacings are negligibly small. We therefore consider only those $\psi_{l,m,n}$'s which lie inside and around the Ewald sphere and assume all others to be zero. With this assumption the problem is overspecified, and we have to use a least-squares technique to find the best possible solution. The actual number of $\psi_{l,m,n}$'s that have to be computed is still quite large. Depending on the electron energy, it varies between a few hundred and a few thousand.

IV. Results.—Calculations were performed for a primary electron beam of unit intensity, incident normally on the [100] face of an Al crystal. In the expansion of the real part of the crystal potential [Eq. (1)], the first 27 terms

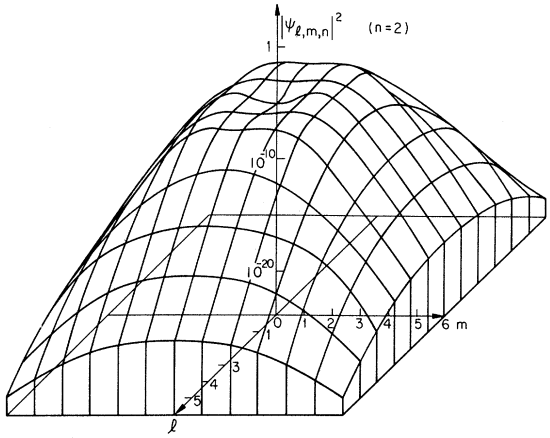

FIG. 1. Expansion coefficients of wave function $\psi(\vec{r})$ in the crystal. Conditions: 40-V electron beam of unit intensity incident normally on [100] face of Al crystal; scattering potential described by a 27-term Fourier expansion (see text). Note: Only the $\psi_{l,m,n}$'s with $l+m$ even are plotted; all $\psi_{l,m,n}$'s with $l+m$ odd are zero due to symmetry of the fcc lattice.

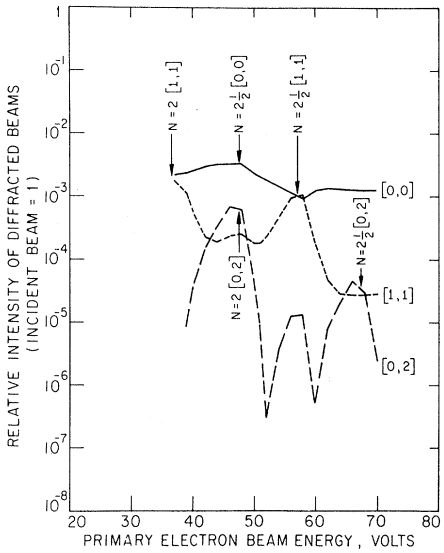

FIG. 2. Beam intensities versus energy. Conditions: Primary beam of unit intensity incident normally on [100] face of Al crystal; same scattering potential as in Fig. 1; the arrows indicate those incident beam energies which give rise to Bragg reflections in the crystal (the inner potential correction is 10 V, as explained in the text); N designates the order of the Bragg peaks, based on a layer spacing $d = 2.02$ Å. Note: beams with "mixed" indices are absent due to symmetry of the fcc lattice.

were considered. The first term [$\mathrm{Re}(w_{0,0,0})$ = 10 V] is the amount of energy the electron gains when it enters the crystal (i.e., the inner potential). This was determined experimentally by observing the energy shift of the Bragg reflection peaks. Because of the symmetry of the fcc lattice, all coefficients $w_{p,q,s}$ with "mixed" indices are zero. The remaining coefficients were calculated by using the method outlined in Ref. 5. The imaginary part of the potential was assumed to be constant, i.e., $\mathrm{Im}[W(\vec{r})] = 2.5$ V.

Figure 1 is a plot of $|\psi_{l,m,n}|^2$ as a function of l and m, on a plane (n = const) in reciprocal space. The distance between the plane and the center of the Ewald sphere is less than one reciprocal lattice spacing. It is seen that $|\psi_{l,m,n}|^2$ drops off very rapidly with increasing indices l and m. Similar graphs are obtained for other sections through the Ewald sphere. Figure 2 shows the intensities of the (0, 0), (1, 1), and (0, 2) beams as a function of electron energy.

V. Conclusions.—First, it has been demonstrated that LEED intensities can be calculated by using Bethe's theory.[5] Second, the calculated curves of intensity versus energy (Fig. 2) show the well-known (integer order) Bragg reflection peaks as well as additional noninteger order peaks, similar to the ones predicted by McRae.[3] Third, it is found that, both inside and outside the crystal, the expansion of the wave function includes many terms whose coefficients are of similar order of magnitude. All these "waves" should be considered, and the "two-beam" treatment appears to be unsatisfactory.

[1]G. Gafner, Surface Sci. 2, 534 (1964).
[2]E. G. McRae and C. W. Caldwell, Surface Sci. 2, 509 (1964).
[3]E. G. McRae, J. Chem. Phys. 45, 3258 (1966).
[4]K. Kirabayashi and Y. Takeishi, Surface Sci. 4, 150 (1966).
[5]H. Bethe, Ann. Physik 87, 55 (1928).

MAGNETIZATION OF THE SUPERCONDUCTING SHEATH

A. S. Joseph, A. C. Thorsen, E. R. Gertner, and J. W. Savage
North American Aviation Science Center, Thousand Oaks, California
(Received 22 May 1967; revised manuscript received 10 November 1967)

Torque measurements on Type-II superconducting foils in nearly parallel applied magnetic fields H indicate that the torque above H_{c2} can provide a direct measure of the magnetization. From the results above H_{c2} we deduce two magnetizations, M_b associated with the bulk sample, and M_S associated only with the superconducting sheath. The measurements indicate that M_S is irreversible with H, contrary to prediction, and that the sheath itself behaves as if it is multiply connected.

Since the theoretical prediction[1] and the experimental verification[2] of a sheath state in Type-II superconductors above the critical field H_{c2}, there has been considerable experimental effort[3] to characterize the properties of the sheath state. In addition, recent theoretical work[4-6] has led to a model of the current distribution in the sheath which has met with some success in explaining magnetization measurements above H_{c2}. This model is shown schematically in Figs. 1(a) and 1(b) for a superconductor of rectangular cross section and of unit length. (In the following discussion we treat the currents in the superconducting sheath as average line currents although of course they have a finite spatial distribution.) Clockwise and counterclockwise currents J_1 and J_2 are predicted to flow perpendicular to the magnetic field H in a region extending a few coherence lengths below the surface. According to the theory, the direction of each current remains fixed for a given applied field direction, while the magnitudes of J_1 and J_2 may change continuously such that the difference $\Delta J = J_1 - J_2$ can be positive or negative depending on whether the field is increasing [Fig. 1(a)] or decreasing [Fig. 1(b)].

In order to facilitate the following discussion we designate the current J_2 which flows around the inner path as J and denote the current J_1 flowing around the outer surface as $J + \Delta J$. The current $J + \Delta J$ encloses the total cross-sectional area of the bulk, A, and the current J encloses the inner area $A - \Delta A$, where ΔA